



Universiteit
Leiden
The Netherlands

The relation between vascular risk factors and flow in cerebral perforating arteries: a 7 Tesla MRI study

Onkenhout, L.; Arts, T.; Ferro, D.; Kuipers, S.; Oudeman, E.; Harten, T. van; ... ; Heart Brain Connection Study Grp

Citation

Onkenhout, L., Arts, T., Ferro, D., Kuipers, S., Oudeman, E., Harten, T. van, ... Kappelle, L. J. (2024). The relation between vascular risk factors and flow in cerebral perforating arteries: a 7 Tesla MRI study. *Cerebrovascular Diseases*, 54(1), 121-128.
doi:10.1159/000537709

Version: Publisher's Version

License: [Creative Commons CC BY 4.0 license](#)

Downloaded from: <https://hdl.handle.net/1887/4195233>

Note: To cite this publication please use the final published version (if applicable).

The Relation between Vascular Risk Factors and Flow in Cerebral Perforating Arteries: A 7 Tesla MRI Study

Laurien Onkenhout^a Tine Arts^b Doeschka Ferro^a Sanne Kuipers^a

Eline Oudeman^{a,c} Thijs van Harten^d Matthias J.P. van Osch^d

Jaco Zwanenburg^b Jeroen Hendrikse^b Geert Jan Biessels^a

L. Jaap Kappelle^a on behalf of the Heart-Brain Connection-Study Group

^aDepartment of Neurology and Neurosurgery, UMC Utrecht Brain Center, University Medical Center Utrecht, Utrecht, The Netherlands; ^bDepartment of Radiology, Center for Image Sciences, University Medical Center Utrecht, Utrecht, The Netherlands; ^cDepartment of Neurology, Franciscus Gasthuis & Vlietland, Rotterdam, The Netherlands; ^dDepartment of Radiology, Leiden University Medical Center, Leiden, The Netherlands

Keywords

Cerebral perforating artery · Flow velocity · Pulsatility · 7 Tesla MRI · Vascular risk factors

Abstract

Introduction: Cerebral perforating arteries provide blood supply to the deep regions of the brain. Recently, it became possible to measure blood flow velocity and pulsatility in these small arteries. It is unknown if vascular risk factors are related to these measures. **Methods:** We measured perforating artery flow with 2D phase-contrast 7 Tesla MRI at the level of the centrum semiovale (CSO) and the basal ganglia (BG) in seventy participants from the Heart Brain Connection study with carotid occlusive disease (COD), vascular cognitive impairment (VCI), or no actual cerebrovascular disease. Vascular risk factors included hypertension, diabetes, hyperlipidemia, and smoking. **Results:** No consistent relations were found between any of the vascular risk factors and either flow velocity or flow pulsatility, although there was a relation between lower diastolic blood pressure and

higher pulse pressure and higher cerebral perforator pulsatility ($p = 0.045$ and $p = 0.044$, respectively) at the BG level. Results were similar in stratified analyses for patients with and without a history of cardiovascular disease, or only COD or VCI. **Conclusion:** We conclude that, cross-sectionally, cerebral perforating artery flow velocity and pulsatility are largely independent of the presence of common vascular risk factors in a population with a mixed vascular burden.

© 2024 The Author(s).
Published by S. Karger AG, Basel

Introduction

Cerebral perforating arteries are distal arterial branches that supply blood to the deep regions of the brain [1]. In healthy people, the flow in these small arteries is kept stable by the vasomotor response, but in elderly people or in participants with cerebrovascular disease, this protective reflex may fail [2, 3]. Recently, it has become possible to visualize cerebral perforating

arteries with 7 Tesla MRI and to perform flow measures on them [3–6]. There is emerging evidence that these flow measures are abnormal in patients with small vessel disease [7]. Yet, it is unknown which factors can affect these flow measures in perforating arteries. From autopsy studies we know that perforating arteries may remodel in the presence of vascular risk factors [8]. Increased oxidative stress, endothelial damage, apoptosis, and inflammation may play a role in this process and as such may cause impaired vascular dilation resulting in altered pulsatility. In large vessels, this phenomenon is an early marker of vascular pathology, even before structural changes to the vascular wall are visible in both pathological and in vivo imaging [8–11].

Studies about the relation between vascular risk factors and flow velocity and pulsatility in large intracranial vessels (i.e., internal carotid arteries, middle cerebral artery) have shown that these vascular risk factors were associated with altered flow velocity and pulsatility. This suggests that these risk factors can lead to altered hemodynamics within the brain [3, 12, 13]. Hypertension has been associated with a decrease in cerebral perfusion and diabetes, hyperlipidemia, and smoking have been associated with higher pulsatile and lower mean flow velocity [3, 9, 14]. Whether these associations also exist in the small perforating artery function is unknown (online suppl. Fig. 1; for all online suppl. material, see <https://doi.org/10.1159/000537709>). The aim of the current cross-sectional study is to investigate the relationship between presence and levels of traditional vascular risk factors (hypertension, diabetes, hyperlipidemia, and smoking) and flow velocity and pulsatility in cerebral perforating arteries in a population with a mixed burden of cerebrovascular disease.

Methods

Study Population

The Heart-Brain Connection (HBC) study is a multicenter study that investigates relationships between (cardio)vascular risk factors, the hemodynamic status of the heart and the brain, and cognitive impairment in four participant categories (carotid occlusive disease [COD], vascular cognitive impairment [VCI], heart failure, and a reference group) [13]. Patients with heart failure were not included in the current study because no 7 Tesla MRI scanning was performed in this group.

For the present 7 Tesla MRI study, 95 participants included between 2019 and 2021 qualified and provided written informed consent. After exclusion of participants with unusable 7 Tesla MRI data at the level of both the centrum semiovale (CSO) and the basal ganglia (BG), due to either participant movement during scanning or erroneous slice planning, data of 70 participants, COD ($n = 24$), VCI ($n = 10$), and reference group ($n = 36$), remained. From the 70

included participants, MRI scans of 10 participants were excluded from analysis at the CSO level due to subject motion. At the BG level, MRI scans of 19 participants could not be analyzed: 7 due to subject motion and 12 due to erroneous slice planning. Information about vascular risk factors was complete in all participants. Patients and controls were matched for age and sex through frequency matching (online suppl. Fig. 2).

Group-specific inclusion and exclusion criteria for the overall HBC study have been described in detail previously [13]. COD was defined as a 100% occlusion of the internal carotid artery assessed with magnetic resonance angiography. VCI and inclusion criteria were cognitive complaints, a Clinical Dementia Rating scale score of ≤ 1 , and a Mini-Mental State Examination score of ≥ 20 (i.e., we included patients with subjective cognitive decline, mild cognitive impairment, or mild dementia). Patients with VCI had moderate to severe vascular disease on MRI, namely white matter lesion (Fazekas >1) and/or lacunar infarct(s) and/or intracerebral (micro)hemorrhage(s); or mild white matter lesions (Fazekas = 1) in combination with at least one vascular risk factor. The participants in the reference group did not have a history COD or VCI.

This study was approved by the Institutional Review Board of the University Hospital Leiden and Utrecht. All patients provided written informed consent. The study was conducted in accordance with the declaration of Helsinki and the medical Research Involving Human Subjects Act (WMO).

Vascular Risk Factors

Blood Pressure

Systolic and diastolic blood pressure (in mm Hg) was acquired in a standardized way. During the study visit, the patient was asked to sit for 5 min, after which the blood pressure was measured on each arm and repeated at least 1 min later. Mean systolic and diastolic blood pressure was averaged out of these four measurements. The pulse pressure was calculated by subtracting the mean diastolic blood pressure from the mean systolic blood pressure. The criteria for hypertension were: use of antihypertensive medication, a mean systolic blood pressure above 140 mm Hg, or a mean diastolic blood pressure above 90 mm Hg.

Diabetes Mellitus Type 2

The criteria for diabetes mellitus type 2 were: use of antidiabetic medication or a diagnosis of diabetes by a physician (even if a patient did not use medication, but, e.g., would adhere to a diet).

Hyperlipidemia

The criteria for hyperlipidemia were: use of cholesterol-lowering medication or a diagnosis of hyperlipidemia by a physician based on earlier blood cholesterol and LDL levels (even if a patient did not use medication, but, e.g., would adhere to a diet) or a present LDL above 3.5 mmol/L.

Smoking

Both current and a history of smoking were noted, as well as the number of pack-years.

7 Tesla MRI Data Acquisition and Processing

7 Tesla MRI data were acquired on a Philips Achieva MRI system in Leiden or Utrecht. Flow velocity and pulsatility in cerebral perforating arteries were measured at two levels: the CSO and the BG [13].

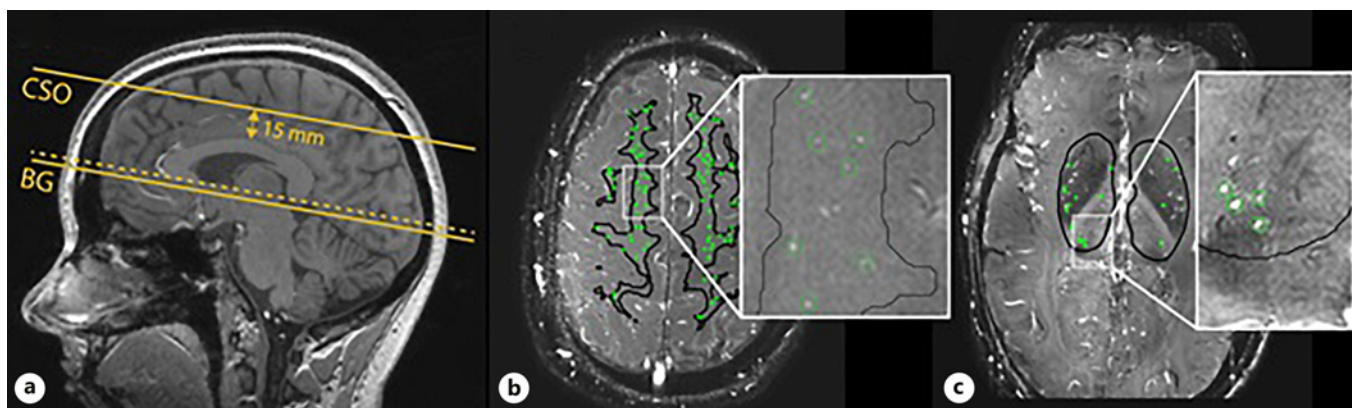


Fig. 1. Planning of the two-dimensional (2D) quantitative flow (Qflow) slices and regions of interest (ROIs). **a** Planning of the BG and CSO slices on a sagittal T1-weighted image. The slice planning is indicated by the yellow lines. For the BG, a 2D slice is planned through the anterior commissure, parallel to the genu aligned to the splenium of the corpus callosum (dotted line) and aligned in the horizontal plane for the left/right axis; CSO planning is parallel

to the BG plane located 15 mm above the corpus callosum. **b** ROI (border indicated by the black line; see methods for details) on the 2D Qflow image in the CSO slice, cerebral perforating arteries detected circled in green. A larger surface area was measured compared to the BG slice and more perforators detected in comparison due to natural anatomy **(c)** ROI in the BG slice, cerebral perforating arteries detected circled in green [15].

Cerebral perforating artery flow velocity and pulsatility 2D phase-contrast (PC) acquisitions were performed on 7T MRI, aimed at small perforating arteries in an axial slice at the level of the CSO (arterial diameter approx. 100–300 μm) and the BG (approx. 200–800 μm). We used a previously published sequence which has been described in more detail elsewhere [4, 5]. In brief, the 2D PC acquisition was time-resolved over the cardiac cycle with the following parameters: $0.3 \times 0.3 \times 2.0 \text{ mm}^3$ resolution, velocity encoding strength (V_{enc}) = 4 cm/s for the CSO, and $V_{\text{enc}} = 20 \text{ cm/s}$ for the BG (online suppl. Table 1; Fig. 1). Slice planning of the PC acquisitions was individually adapted, based on a T1 image. A peripheral pulse oximeter was used for retrospective gating and cushions were placed beside the subject's head to minimize head movement during scanning.

Perforating artery flow was assessed within a 2D white matter mask at the CSO level and a manually delineated 2D mask at the BG level, both excluding infarcts [13]. White matter masks and infarcts in these regions were delineated from 3 Tesla MRI T1-weighted and FLAIR images with the Quantib Brain Segmentation Tool (FSL version 6.0.1, Oxford, UK). Registration of these masks to 7 Tesla space was done with FMRIB Software Library (FSL version 6.0.1, Oxford, UK). The infarct masks were dilated with a $3 \times 3 \text{ mm}$ kernel. Only the central white matter (further than 16 mm away from the outer rim of the brain on the PC slice) was included because the poor gray/white matter contrast in these regions on the PC image makes it difficult to recognize inclusion of gray matter into the white matter mask. The assessed slice of the CSO and BG is based on the field of view of the specific slice, which is $250 \times 250 \text{ mm}$ at the CSO level and $250 \times 169 \text{ mm}$ at the BG level; each slice is 2.0 mm thick.

Cerebral perforating arteries in the CSO and BG were detected as previously published, also automatically excluding CSO perforating arteries located in regions with ghosting artifacts and perforating arteries in the BG oriented nonperpendicularly to the scanning plane [10]. In brief, the algorithm identifies perforating

arteries by pixels with a mean velocity over the cardiac cycle that is significantly different from the static background tissue. In addition, apparent perforating arteries located within a 1.2-mm radius from each other were excluded, as these are mostly “false detections” located on larger and nonperpendicular vessels.

Blood flow velocity (cm/s) and pulsatility ($(V_{\text{max}} - V_{\text{min}}) / V_{\text{mean}}$, based on the normalized velocity curves) were assessed by averaging over all detected cerebral perforating arteries [5, 10]. Perforating artery count within the regions of interest was expressed as a density (N_{density} , the number of perforating arteries per cm^2 mask).

Statistical Analysis

Data are presented as mean \pm SD or proportions, as appropriate. The relations between the vascular risk factors and perforating artery flow and pulsatility were assessed with linear regression analyses, adjusted for age and sex, and presented as an unstandardized beta {B [95% confidence interval {CI}]} for dichotomous risk factors (i.e., hypertension, diabetes mellitus type 2, hyperlipidemia, and current or previous smoker) and as a standardized beta (B [95% CI]) for continuous risk factor measures (i.e., systolic and diastolic blood pressure and pulse pressure, HbA1c and LDL cholesterol).

Additional analyses addressed the presence of one or more risk factors (0 vs. ≥ 1 and 0 vs. ≥ 2 ; independent of the type of risk factor). In sensitivity analyses, to rule out that our findings were driven by a clinical manifestation of vascular pathology, we performed three post hoc analyses: first excluding 37 participants with a history of transient ischemic attack or ischemic stroke, or cardiovascular disease defined as angina pectoris, ischemic heart disease, dotter treatment, bypass, or peripheral arterial disease; second, with analyses only including the COD group; and third, with only including the VCI group. Adjusting for multiple comparisons was not conducted since all analyses were exploratory, also due to the limited significant findings; therefore, there

Table 1. Demographics, MRI features, and vascular risk factors ($N = 70$)

Demographics	
Age, years	65±8
Male sex (%)	44 (63)
Group	
COD (%)	24 (34.3)
VCI (%)	10 (14.3)
Controls (%)	36 (51.4)
Vascular risk factors	
Hypertension (%)	37 (53)
Systolic blood pressure, mm Hg	140±20
Diastolic blood pressure, mm Hg	83±11
Pulse pressure, mm Hg	57±14
Hyperlipidemia (%)	41 (59)
LDL cholesterol, mmol/L	3.1±1.0
Type 2 diabetes (%)	7 (10)
HbA1c, mmol/mol	38±5.9
Current smoking/pack-years	10 (14)/31±16
History of smoking/pack-years	41 (59)/24±23
Perforating artery measures	
No. of perforating arteries detected CSO ($N = 60$)	36±20
No. of perforating arteries detected BG ($N = 51$)	16±5
N_{density} of CSO (# perforating arteries/cm ²) ($N = 60$)	2.4±1.0
N_{density} of BG (# perforating arteries/cm ²) ($N = 51$)	0.7±0.2
Pulsatility (PI) CSO ($N = 60$)	0.43±0.16
Pulsatility (PI) BG ($N = 51$)	0.42±0.14
Flow velocity CSO, cm/s ($N = 60$)	0.71±0.16
Flow velocity BG, cm/s ($N = 51$)	3.7±0.75

Data are presented as mean ± standard deviation or as N (%). COD, carotid occlusive disease; VCI, vascular cognitive impairment; CSO, centrum semiovale; BG, basal ganglia; N , number.

was no need to protect against false positives. Medication use was not taken into account in the analyses in this explorative study. Data analyses were performed in IBM SPSS statistics (v. 22, SPSS Inc., Chicago, IL, USA). A p value ≤ 0.05 was considered statistically significant.

Results

Fifty-three percent of the 70 participants had hypertension, 59% had hyperlipidemia, 10% had diabetes mellitus type 2, 14% were current smokers, and 59% had a history of smoking (Table 1). At the CSO and at the BG level, the mean number of detected cerebral perforating arteries was 36 ± 20 and 16 ± 5 , respectively. None of the vascular risk factors was related to the density of perforating arteries at the CSO nor at the BG level (data not shown).

No consistent relations were found between the presence of any of the vascular risk factors and either flow velocity or pulsatility at the CSO or BG level (Table 2). At the BG level, an association was found between higher

diastolic blood pressure and (1) lower cerebral perforator pulsatility (standardized beta: -0.29 , 95% CI: -0.57 to -0.01 ; $p = 0.045$) and (2) lower flow velocity (standardize beta: -0.26 , 95% CI: -0.52 to 0.00 ; $p = 0.052$) and also between higher pulse pressure and a higher cerebral perforator pulsatility (beta: 0.30 , 95% CI: 0.01 – 0.59 ; $p = 0.044$).

In the prespecified additional analyses, we did not find a relation between the presence of multiple vascular risk factors (regardless of type) and measures of perforating artery flow (Table 3). The three subgroups showed no significant differences in either flow velocity or pulsatility in the CSO or in the BG (online suppl. Table 2).

Discussion

We did not observe consistent relations between the presence or level of individual vascular risk factors and flow velocity and pulsatility in cerebral perforating

Table 2. Relationship between vascular risk factors and cerebral perforating artery flow

Vascular risk factor	Pulsatility index CSO N = 60	p value	Pulsatility index BG N = 51	p value	Flow velocity CSO (cm/s) N = 60	p value	Flow velocity BG (cm/s) N = 51	p value
Hypertension ^a	-0.02 [-0.10 to 0.06]	0.63	0.00 [-0.08 to 0.08]	0.96	-0.01 [-0.09 to 0.08]	0.88	-0.32 [-0.72 to 0.07]	0.11
Systolic blood pressure	-0.14 [-0.41 to 0.13]	0.30	-0.03 [-0.33 to 0.28]	0.87	-0.03 [-0.31 to 0.25]	0.84	-0.22 [-0.50 to 0.07]	0.14
Diastolic blood pressure	-0.19 [-0.44 to 0.07]	0.16	-0.29 [-0.57 to -0.01]	0.045*	0.05 [-0.22 to 0.32]	0.70	-0.26 [-0.52 to 0.00]	0.052
Pulse pressure	0.13 [-0.14 to 0.40]	0.14	0.30 [0.01-0.59]	0.044*	-0.04 [-0.32 to 0.25]	0.79	-0.01 [-0.30 to 0.27]	0.94
Diabetes mellitus type 2 ^a	0.02 [-0.13 to 0.18]	0.75	0.10 [-0.03 to 0.23]	0.12	-0.09 [-0.25 to 0.07]	0.24	-0.04 [-0.72 to 0.64]	0.90
HbA1c	0.17 [-0.09 to 0.43]	0.19	-0.01 [-0.30 to 0.29]	0.95	0.04 [-0.23 to 0.31]	0.76	0.02 [-0.25 to 0.30]	0.86
Hyperlipidemia ^a	0.02 [-0.06 to 0.10]	0.63	0.03 [-0.05 to 0.11]	0.48	-0.04 [-0.13 to 0.05]	0.39	-0.26 [-0.68 to 0.17]	0.23
LDL cholesterol	0.02 [-0.25 to 0.28]	0.87	-0.19 [-0.50 to 0.12]	0.22	-0.08 [-0.35 to 0.20]	0.58	0.18 [-0.11 to 0.47]	0.21
Current or previous smoker ^a	-0.00 [-0.12 to 0.12]	0.96	0.03 [-0.07 to 0.12]	0.59	-0.11 [-0.23 to 0.02]	0.09	-0.17 [-0.67 to 0.33]	0.50

Continuous data are presented as a standardized beta [95% CI]. CSO, centrum semiovale; BG, basal ganglia. ^aDichotomous data are presented as an unstandardized beta [95% CI]. All data are adjusted for age and sex. $p < 0.05$ was considered significant and marked*.

Table 3. Relationship between the presence of one or more vascular risk factor(s) and cerebral perforating artery flow

Vascular risk factor	Pulsatility index CSO N = 60	p value	Pulsatility index BG N = 51	p value	Flow velocity CSO (cm/s) N = 60	p value	Flow velocity BG (cm/s) N = 51	p value
Presence of one risk factor compared to none	-0.01 PI [-0.13 to 0.11]	0.82	-0.03 PI [-0.15 to 0.09]	0.57	-0.05 cm/s [-0.18 to 0.08]	0.42	-0.07 cm/s [-0.68 to 0.53]	0.83
Presence of two or more risk factors compared to none	0.01 PI [-0.08 to 0.09]	0.86	0.00 PI [-0.08 to 0.09]	0.93	-0.04 cm/s [-0.13 to 0.05]	0.37	-0.35 cm/s [-0.79 to 0.09]	0.12

CSO, centrum semiovale; BG, basal ganglia. Data in the presence of risk factor are dichotomous and presented as an unstandardized beta [95% confidence interval]. All data are corrected for age and sex. $p < 0.05$ was considered significant and marked*.

arteries. Prior studies that investigated the relation between blood pressure, diabetes mellitus type 2, (LDL) cholesterol and smoking, and functional measures of large intracranial vessels, i.e., internal carotid artery and primary branches of the circle of Willis, found that these

risk factors are associated with changes of the blood pulsatility and decreased flow velocity [9, 11, 14]. A study of ultrasound and CT angiography of the carotid artery has shown that the presence of vascular risk factors is associated with reduced blood flow velocity, increased

pulsatility, and impaired cerebrovascular reactivity [11]. Common vascular risk factors are associated with increased pulse pressure indicating arterial stiffness, and decreased blood flow in the middle cerebral artery [16–18]. Several MRI studies with arterial spin labeling have demonstrated that vascular risk factors may be associated with overall reduced cerebrovascular perfusion [9, 19–21].

Our observed values for perforating artery flow velocity and pulsatility in the CSO and BG are largely in agreement with previous literature, and only velocities in the BG are slightly lower but not significant [4–6]. The number of detected perforating arteries in our study was lower than previously reported, probably due to more rigorous exclusion of nonperpendicular perforating arteries in the BG and the exclusion of perforating arteries located in ghosting regions in the CSO. The exclusion of nonperpendicular perforating arteries at the level of the BG may also explain why velocities in that region are slightly lower than in previous studies [4–6] because nonperpendicular perforating arteries are somewhat larger with higher blood flow velocities. This approach of the perforating arteries gives better and more specified results, since measurements in nonperpendicular arteries can be unreliable.

Hypertension is known to induce adaptive changes in cerebral arteries such as hypertrophy in smooth muscle cells, impaired endothelial function, increase of the vascular wall thickness, and vasomotor dysfunction [22, 23]. Hyperlipidemia, type 2 diabetes, and smoking are also associated with endothelial dysfunction [24, 25]. Furthermore, diabetes mellitus type 2 and specifically the associated hyperglycemia are considered major stimuli for oxidative stress and are associated with increased inflammation [24, 25].

We can only speculate about why consistency is lacking in the relation between vascular risk factors and cerebral artery flow measurements. First, we investigated a patient population that received strict cardiovascular risk management, which overall may have limited the effect of these risk factors (online suppl. Table 2, specifications per group) on the cerebral perforating arteries. Nevertheless, in post hoc analyses, we also did not observe any relation between vascular risk factors and cerebral artery flow measurements in participants without a prior cerebrovascular event. Treatment of vascular risk factors and lifestyle modifications, such as medical treatments, smoking cessation, weight loss, diet change, and exercise, is known to be effective in (partially) reversing its damaging effects on the vessel wall [14]. These treatment effects are

dependent on the severity of the vascular diseases. Second, all participants in this study were able to participate in the study and could undergo a 7T MRI scan, arguing that we have studied participants in a relatively good condition with stable blood flow velocity and pulsatility. Finally, it could be that hypertension activates autoregulation mechanisms to stabilize cerebral blood flow [23, 26, 27]. Autoregulation mechanisms involve neurovascular coupling in which endothelium regulates vasodilation and vasoconstriction to ensure appropriate cerebral blood flow resulting in stable flow velocity and pulsatility [27]. The same may hold true for hyperlipidemia, diabetes, and smoking [14, 25]. The effect sizes we found were consistent in BG and CSO except for diastolic blood pressure and pulse pressure for which we found a small statistical significant effect at the BG but not at the CSO level. Our results show that at the BG level, higher diastolic blood pressure is associated with lower pulsatility and that a higher pulse pressure is associated with higher pulsatility. An elevated diastolic blood pressure is likely indicative of an accompanying decrease in pulse pressure. Pulsatility can increase depending on the stage of vascular alterations, but can also decrease as a result of cerebral vascular alterations [9, 11, 14]. Pulse pressure is an indication of arterial stiffness, higher pulse pressure indicating more arterial stiffness and therefore higher pulsatility [28]. Vessel dilatation can lead to lowered pulsatility if vascular reactivity is intact [29]. That we only find this at the BG level might be caused by the fact that the perforating arteries at the CSO level are smaller than the more proximally located arteries at the BG level. Therefore, the CSO level is further from the main cerebral arteries and the vascular system may have had a longer trajectory to carry out the compensating mechanisms.

It is relevant to mention that while our study focused on the relation between vascular risk factors and cerebral perforating artery measures, there are observations regarding other influential factors such as downstream large vessel atherosclerosis. Notably, in a previous study with 7 Tesla MRI, it was observed that measures of cerebral perforating artery flow largely remained consistent in patients with COD [15]. Focusing on upstream, previous studies have looked at the relationship between cerebral brain perfusion and WMH severity. However, their outcomes were inconsistent, which means that establishing causality remains a challenge. Moreover, cerebral brain perfusion cannot be directly compared to cerebral perforating artery measures. Further research is required to understand this relationship in depth.

An important strength of this study is the relatively large sample size of participants who underwent a 7 Tesla MRI allowing the measurements in such small perforators. In addition, we measured cerebral perforating artery flow at two brain levels, i.e., the CSO and BG, which are both fed by different arteries, allowing us to distinguish between these two brain regions and its place in the vascular tree.

Some limitations of our study need to be considered. First, during scanning the PC sequence is relatively sensitive for motion. This may result in motion artifacts and, as such, in unreliable velocity and pulsatility measurements. Therefore, a number of MRI scans could not be assessed due to movement artifacts, even though the participants were instructed to lie as still as possible. These dropout numbers are known from previous similar studies on 7 Tesla MRI and are inherent to the complexity and sensitivity of the scanning method. The same can be said for erroneous planning of the sequences [3, 5]. Since the presence of the different vascular risk factors was more or less evenly distributed between dropouts and participants, this probably did not cause selection bias. Second, the heterogeneity of our population may have affected our findings, as their underlying pathology is different, e.g., in participants with severe atherosclerotic large vessel disease, or in those with cerebral small vessel disease. However, sensitivity analyses addressing this heterogeneity showed similar results. Third, it is important to acknowledge the absence of specified data on participant use of medications that may influence the cardiovascular system. Therefore, we are unsure of possible mitigating effects of such drugs on the relationship between risk factors and perforating artery function. Lastly a possible limitation is that we did not have real-time laboratory measurements such as blood glucose, that may influence blood viscosity and flow dynamics, at the time of the 7T MRI scans. In conclusion, this study indicates that blood flow velocity and pulsatility of cerebral perforating arteries are largely independent of the concurrent presence or level of vascular risk factors in a population above the age of 50 years with mixed vascular burden.

Acknowledgments

This work is part of the Heart-Brain Connection crossroads (HBCx) consortium of the Dutch CardioVascular Alliance (DCVA). We acknowledge the support from European Union Horizon2020 projects SVDs@target and SELMA; Dutch Federa-

tion of University Medical Centers; the Netherlands Organisation for Health Research and Development; and the Royal Netherlands Academy of Sciences. The work at the LUMC has been made possible by the Dutch Heart Foundation and the Netherlands Organisation for Scientific Research (NWO), as part of their joint strategic research program: “Earlier recognition of cardiovascular diseases.”

Statement of Ethics

This study was conducted in compliance with the guidelines for human studies and in accordance with the World Medical Association Declaration of Helsinki. All subjects have given their written informed consent. This study protocol was reviewed and approved by Ethics Board of the University Medical Center Utrecht and Leiden (approval number 14-493C).

Conflict of Interest Statement

The authors declare that they have no conflict of interest.

Funding Sources

HBCx has received funding from the Dutch Heart Foundation under Grant agreements 2018-28 and CVON 2012-06. We acknowledge the support from European Union Horizon2020 projects SVDs@target (No. 66688) and SELMA (No. 841865).; This project is partially financed by the PPP Allowance made available by Top Sector Life Sciences & Health to the Dutch Heart foundation to stimulate public-private partnerships.

Author Contributions

L.P. Onkenhout: study concept and design, data acquisition, analysis and interpretation of the data, and drafting the manuscript. T. Arts: study concept and design, data acquisition, and critical revision of the manuscript. S. Kuipers: data acquisition and critical revision of the manuscript. E.A. Oudeman, D.A. Ferro, T. van Harten, M.J.P. van Osch, and J.J.M. Zwanenburg: data acquisition and critical revision of the manuscript. J. Hendrikse: study concept and design, and critical revision of the manuscript. G.J. Biessels and L.J. Kappelle: study concept and design, obtaining funding, interpretation of the data, and revising the manuscript for important intellectual content.

Data Availability Statement

All data analyzed during this study are included in this article and its online supplementary material files. Further inquiries can be directed to the corresponding author.

References

- Chandra A, Li W, Stone C, Geng X, Ding Y. The cerebral circulation and cerebrovascular disease I: anatomy. *Brain Circ.* 2017;3(2):45–56.
- Wardlaw JM, Smith C, Dichgans M. Mechanisms of sporadic cerebral small vessel disease: insights from neuroimaging. *Lancet Neurol.* 2013;12(5):483–97.
- Geurts LJ, Zwanenburg JJM, Klijn CJM, Luijten PR, Biessels GJ. Higher pulsatility in cerebral perforating arteries in patients with small vessel disease related stroke, a 7T MRI study. *Stroke.* 2019;50(1):62–8.
- Bouvy WH, Geurts LJ, Kuijff HJ, Luijten PR, Kappelle LJ, Biessels GJ, et al. Assessment of blood flow velocity and pulsatility in cerebral perforating arteries with 7-T quantitative flow MRI. *NMR Biomed.* 2016;29(9):1295–304.
- Geurts L, Biessels GJ, Luijten P, Zwanenburg J. Better and faster velocity pulsatility assessment in cerebral white matter perforating arteries with 7T quantitative flow MRI through improved slice profile, acquisition scheme, and postprocessing. *Magn Reson Med.* 2018;79(3):1473–82.
- Schnerr RS, Jansen JFA, Uludag K, Hofman PAM, Wildberger JE, van Oostenbrugge RJ, et al. Pulsatility of lenticulostriate arteries assessed by 7 Tesla flow MRI-Measurement, reproducibility, and applicability to aging effect. *Front Physiol.* 2017;8:961.
- van den Brink H, Kopczak A, Arts T, Onkenhout L, Siero JCW, Zwanenburg JJM, et al. CADASIL affects multiple aspects of cerebral small vessel function on 7T-MRI. *Ann Neurol.* 2023;93(1):29–39.
- Granger DN, Rodrigues SF, Yildirim A, Senchenkova EY. Microvascular responses to cardiovascular risk factors. *Microcirculation.* 2010;17(3):192–205.
- Pase MP, Grima NA, Stough CK, Scholey A, Pipingas A. Cardiovascular disease risk and cerebral blood flow velocity. *Stroke.* 2012;43(10):2803–5.
- Arts T, Siero JCW, Biessels GJ, Zwanenburg JJM. Automated assessment of cerebral arterial perforator function on 7T MRI. *J Magn Reson Imaging.* 2021;53(1):234–41.
- Bai CH, Chen JR, Chiu HC, Pan WH. Lower blood flow velocity, higher resistance index, and larger diameter of extracranial carotid arteries are associated with ischemic stroke independently of carotid atherosclerosis and cardiovascular risk factors. *J Clin Ultrasound.* 2007;35(6):322–30.
- Webb AJS, Simoni M, Mazzucco S, Kuker W, Schulz U, Rothwell PM. Increased cerebral arterial pulsatility in patients with leukoaraiosis: arterial stiffness enhances transmission of aortic pulsatility. *Stroke.* 2012;43(10):2631–6.
- Hooghiemstra AM, Bertens AS, Leeuwis AE, Bron EE, Bots ML, Brunner-La Rocca HP, et al. The missing link in the pathophysiology of vascular cognitive impairment: design of the heart-brain study. *Cerebrovasc Dis Extra.* 2017;7(3):140–52.
- Petrie JR, Guzik TJ, Touyz RM. Diabetes, hypertension, and cardiovascular disease: clinical insights and vascular mechanisms. *Can J Cardiol.* 2018;34(5):575–84.
- Onkenhout LP, Arts T, Ferro D, Oudeman EA, van Osch MJP, Zwanenburg JJM, et al. Perforating artery flow velocity and pulsatility in patients with carotid occlusive disease. A 7 tesla MRI study. *Cereb Circ Cogn Behav.* 2022;3:100143.
- Rundek T, Sacco RL, Boden-Albala B. Relationship of carotid and middle cerebral artery pulsatility indices and risk factors for stroke. *Stroke.* 1998;29(2):371–5.
- Vigen T, Ihle-Hansen H, Lyngbakken MN, Berge T, Thommessen B, Ihle-Hansen H, et al. Carotid atherosclerosis is associated with middle cerebral artery pulsatility index. *J Neuroimaging.* 2020;30(2):233–9.
- Kato T, Yoshimura S, Nomura S. Pulsatility of the middle cerebral artery and risk factors associated with intracranial arteriosclerosis. *Stroke.* 2006;37(5):1175–9.
- Jefferson AL, Cambronero FE, Liu D, Moore EE, Neal JE, Terry JG, et al. Higher aortic stiffness is related to lower cerebral blood flow and preserved cerebrovascular reactivity in older adults. *Circulation.* 2018;138(18):1951–62.
- Cho SJ, Sohn YH, Kim GW, Kim JS. Blood flow velocity changes in the middle cerebral artery as an index of the chronicity of hypertension. *J Neurol Sci.* 1997;150(1):77–80.
- Kwater A, Gasowski J, Gryglewska B, Wizner B, Grodzicki T. Is blood flow in the middle cerebral artery determined by systemic arterial stiffness? *Blood Press.* 2009;18(3):130–4.
- Neumann S, Burchell AE, Rodrigues JCL, Lawton CB, Burden D, Underhill M, et al. Cerebral blood flow response to simulated hypovolemia in essential hypertension a magnetic resonance imaging study. *Hypertension.* 2019;74(6):1391–8.
- Pires PW, Dams Ramos CM, Matin N, Dorrance AM. The effects of hypertension on the cerebral circulation. *Am J Physiol Heart Circ Physiol.* 2013;304(12):H1598–614.
- Pruzin JJ, Nelson PT, Abner EL, Arvanitakis Z. Review: relationship of type 2 diabetes to human brain pathology. *Neuropathol Appl Neurobiol.* 2018;44(4):347–62.
- Lekakis J, Papamichael C, Vemmos C, Stamatelopoulos K, Voutsas A, Stamatelopoulos S. Effects of acute cigarette smoking on endothelium-dependent arterial dilatation in normal subjects. *Am J Cardiol.* 1998;81(10):1225–8.
- Iadecola C, Davisson RL. Hypertension and cerebrovascular dysfunction. *Cell Metab.* 2008;7(6):476–84.
- Faraci FM, Heistad DD. Regulation of large cerebral arteries and cerebral microvascular pressure. *Circ Res.* 1990;66(1):8–17.
- Mitchell GF. Arterial stiffness and wave reflection: biomarkers of cardiovascular risk. *Artery Res.* 2009;3(2):56–64.
- Leyden JWC. Cerebral autoregulation and pulsatility: a review. *Front Neurol.* 2016;7:8.